Combined Effects of Fe$_3$O$_4$ Nanoparticles and Chemotherapeutic Agents on Prostate Cancer Cells In Vitro

Kanako Kojima [1], Sanai Takahashi [1], Shungo Saito [1], Yoshihiro Endo [1], Tadashi Nittami [1], Tadashige Nozaki [2], Ranbir Chander Sobti [3,4] and Masatoshi Watanabe [1,5,*]

[1] Laboratory for Medical Engineering, Division of Materials Science and Chemical Engineering, Graduate School of Engineering, Yokohama National University, Yokohama Kanagawa 240-8501, Japan; kana51.minnie93@gmail.com (K.K.); sanai.takahashi@gmail.com (S.T.); springfive.3110@gmail.com (S.S.); ortho_meta_para@icloud.com (Y.E.); nittami@ynu.ac.jp (T.N.)
[2] Department of Pharmacology, Faculty of Dentistry, Osaka Dental University, Hirakata, Osaka 573-1121, Japan; nozaki@cc.osaka-dent.ac.jp
[3] Department of Biotechnology, Panjab University, Chandigarh 160014, India; rcsobti@bbau.ac.in
[4] Vice Chancellor BBA (Central) University, Lucknow 226027, India
[5] Department of Oncologic Pathology, Graduate School of Medicine, Mie University, Tsu, Mie 514-8507, Japan
* Correspondence: mawata@doc.medic.mie-u.ac.jp or mawata@ynu.ac.jp; Tel.: +81-59-231-5010

Abstract: Patients with metastatic castration-resistant prostate cancer (mCRPC) have poor outcomes. Docetaxel (DTX)-based therapy is a current standard treatment for patients with mCRPC. Approaches combining conventional chemotherapeutic agents and nanoparticles (NPs), particularly iron oxide NPs, may overcome the serious side effects and drug resistance, resulting in the establishment of new therapeutic strategies. We previously reported the combined effects of Fe$_3$O$_4$ nanoparticles (Fe$_3$O$_4$ NPs) with DTX on prostate cancer cells in vitro. In this study, we investigated the combined effects of Fe$_3$O$_4$ NPs and rapamycin or carboplatin on prostate cancer cells in vitro. Treatment of DU145 and PC-3 cells with Fe$_3$O$_4$ NPs increased intracellular reactive oxygen species (ROS) levels in a concentration-dependent manner. Treatment of both cell lines with 100 μg/mL Fe$_3$O$_4$ NPs for 72 h resulted in significant inhibition of cell viability with a different inhibitory effect. Combination treatments with 100 μg/mL Fe$_3$O$_4$ NPs and 10 μM carboplatin or 10 nM rapamycin in DU145 and PC-3 cells significantly decreased cell viability. Synergistic effects on apoptosis were observed in PC-3 cells treated with Fe$_3$O$_4$ NPs and rapamycin and in DU145 cells with Fe$_3$O$_4$ NPs and carboplatin. These results suggest the possibility of combination therapy with Fe$_3$O$_4$ NPs and various chemotherapeutic agents as a novel therapeutic strategy for patients with mCRPC.

Keywords: prostate cancer; Fe$_3$O$_4$ nanoparticles; carboplatin; rapamycin; reactive oxygen species

1. Introduction

Prostate cancer is the most commonly diagnosed malignancy and the second leading cause of cancer mortality in men in Western countries [1]. Current management options for prostate cancer include watchful waiting, surgery, cryosurgery, radiation therapy, hormonal therapy, and chemotherapy. Choosing the best treatment for localized or locally advanced prostate cancer is based on the age, stage, grade of the tumor, general health and evaluation of the risk and benefit. Because prostate cancer cell growth is dependent on androgen, androgen-deprivation therapy (ADT) is used for men with advanced disease and results in suppression of the disease for many years. However, long-term ADT results in progression to a stage referred to as castration-resistant prostate cancer (CRPC), which may present as either a continuous rise the serum prostate-specific antigen (PSA)

levels, the progression of pre-existing disease, and/or the occurrence of metastatic disease. Treatments for patients with CRPC have changed dramatically with the development of drugs targeting the androgen receptor axis (abiraterone and enzalutamide) and a new taxane (cabazitaxel) [2]. However, docetaxel (DTX)-based chemotherapy is now considered the standard treatment for patients with CRPC and detectable metastatic disease. The current regimen requires administration of high doses of DTX, which induces toxic reactions; thus, combination of DTX with other agents is difficult. Acquired resistance to DTX-based therapy has also been observed [3]. To improve the survival and quality of life of patients with CRPC, it is necessary to modify classical chemotherapies and develop new combination therapies, as well as develop novel therapeutic strategies targeting the molecular basis of CRPC.

Nanomaterials, which are at the leading edge of the developing field of nanotechnology, offer great potential in medicine and pharmacology. Among nanomaterials, nanoparticles (NPs) are defined as ranging in length from 1 to 100 nm in two or three dimensions and show different properties from those of the bulk material [4]. Among various types of NPs, iron oxide (Fe_3O_4 and γ-Fe_2O_3) NPs, which have biocompatible and superparamagnetic properties, appear particularly promising. Importantly, NPs exhibit the superparamagnetism phenomenon, i.e., they become magnetized up to their saturation magnetization in an external magnetic field but do not exhibit any residual magnetic interaction out of the magnetic field [5]. These magnetic iron oxide NPs have immense potential in a variety of biomedical applications, such as drug delivery, magnetofection, hyperthermia, and magnetic resonance imaging [5]. In addition to these properties, these NPs have been shown to have cytotoxicity in cancer cells [6,7]. Combination of Fe_3O_4 NPs with chemotherapeutic agents has been also applied for leukemia, lung cancer, pancreatic cancer, and prostate cancer cells [8–12]. However, Fe_3O_4 NPs had little or no effect on normal cells as same as previous studies [6,12]. In addition, combined application of Fe_3O_4 NPs with other chemotherapeutic drugs may pave the way for reuse of chemotherapeutic drugs, such as platinum compounds and mammalian target of rapamycin (mTOR) inhibitors.

In this study, we aimed to clarify the combined effects of Fe_3O_4 NPs and chemotherapeutic agents (rapamycin and carboplatin) for prostate cancer cell growth in vitro.

2. Materials and Methods

2.1. NP Solution Preparation and Chemical Agents

Fe_3O_4 NPs were obtained from the Toda Kogyo Corporation (Otake, Hiroshima, Japan), and the partial characteristics of these NPs were reported previously [12]. The characterization of Fe_3O_4 NPs by X-ray diffraction (XRD) (RINT-2500, Rigaku, Akishima, Tokyo, Japan) and transmission electron microscopy (TEM) (JEM-1200EX, JEOL, Akishima, Tokyo, Japan) were as follows: The mean XRD size in powder was 9.3 nm, and the mean size of the spherical NPs was about 10 nm, as determined by TEM. Fe_3O_4 NPs showed a hydrodynamic diameter of 83.4 $\pm$ 16.2 nm, possessed a negative surface charge, and exhibited a zeta potential of -40 mV at pH 9.2 and a polydispersity index of 0.19 in deionized water. After ultraviolet-sterilization of the particles, Fe_3O_4 NPs stock suspensions were prepared by suspension of particles in RPMI-1640 (Thermo Fisher Scientific, Waltham, MA, USA) at each concentration of interest (1, 10 and 100 µg/mL), followed by sonication at 30 W for 10 min with an Ultrasonic HomogenizerVP-050 (TAITAEC, Koshigaya, Saitama, Japan). The mean hydrodynamic diameters of Fe_3O_4 NPs were 196.9, 199.5 and 244.7 nm at 1, 10 and 100 µg/mL in culture medium at pH 7.4, respectively. Docetaxel and rapamycin were purchased from Sigma-Aldrich (St. Louis, MO, USA), and carboplatin was purchased from Bristol-Myers Squibb (Tokyo, Japan). These compounds were dissolved in dimethyl sulfoxide (DMSO) (Nacalai Tesque, Kyoto, Japan). The DMSO concentration in the cell culture did not exceed 0.1%.

2.2. Cell Lines

The prostate cancer cell lines DU145 and PC-3 were purchased from American Tissue Type Culture Collection (Manassas, VA, USA) and cultured in RPMI-1640 medium (Thermo Fisher Scientific, Waltham, MA, USA) with 10% fetal bovine serum (FBS) (Sigma-Aldrich, St. Louis, MO, USA) and 100 U/mL penicillin-streptomycin (Thermo Fisher Scientific, Waltham, MA, USA) in 5% CO_2 at 37 °C.

2.3. Flow Cytometry (FCM) Analysis for Fe_3O_4 NPs Uptake by Prostate Cancer Cells

Cells were treated with various concentrations of Fe_3O_4 NPs for 24 h, trypsinized, and suspended in medium. Fe_3O_4 NPs uptake was analyzed using FCM (Merck Millipore, Darmstadt, Germany) according to previous reports [13,14]. Forward-scattered (FS) and side-scattered (SS) light were proportional to cell size and intracellular density of Fe_3O_4 NPs, respectively, and 30,000 cells were measured per sample.

2.4. Measurement of Intracellular Reactive Oxygen Species (ROS)

CM-H_2DCFDA assays (Invitrogen, Carlsbad, CA, USA) were carried out according to the manufacturer's instructions. The desired Fe_3O_4 NPs amounts were added to PC-3 or DU145 cells in the wells and incubated for an additional 24 h at 37 °C (5% CO_2). A fresh stock solution of CM-H_2DCFDA (10 mM) was prepared in phosphate-buffered saline (PBS) (Nacalai Tesque, Kyoto, Japan) and diluted to a final concentration of 1.67 μM in PBS. Cells were washed with PBS, followed by incubation with 50 μL working solution of the fluorochrome marker CM-H_2 DCFDA for 30 min. Fluorescent imaging was recorded using an IX2N-FL-1 microscope (Olympus, Tokyo, Japan) and analyzed using imaging software (Photoshop Elements 8, Adobe Systems, Tokyo, Japan). Treatment with H_2O_2 (100 μM) for 24 h was used as the positive control for intracellular ROS production.

2.5. FCM Analysis for the Cell Cycle

Cells were seeded in 100-mm culture dishes (1×10^6 cells/dish) and then either left untreated (control) or treated with Fe_3O_4 NPs (1, 10 or 100 μg/mL) for 24 h. Cell cycle analysis was conducted using a Cell Cycle Phase Determination Kit (Cayman Chemical Company, Ann Arbor, MI, USA). Samples were analyzed using a Guava EasyCyte HT system (Merck Millipore).

2.6. Alamar Blue Assay for Cell Viability

To determine cell viability, alamarBlue (Alamar Biosciences, Sacramento, CA, USA) was used. The assays were carried out according to the manufacturer's instructions. Briefly, cells were seeded in 24-well plates (1×10^4 cells/well), and the desired Fe_3O_4 NPs amounts and chemotherapeutic drug were added to the wells. Cells were then incubated for an additional 72 h at 37 °C (5% CO_2). AlamarBlue was added to each well at 10% volume and incubated for 200 min. Metabolically active cells reduced the dye into a fluorescent form, and this fluorescent emission signal was measured using a plate reader (excitation/emission: 570/600 nm; Viento XS, DS Pharma Biomedical, Suita, Osaka, Japan). The emission signal was used to estimate cell viability by linear interpolation between the emission from cells treated with 0.1% saponin (0% viability) and that from untreated cells (100% viability).

2.7. FCM Analysis for Cell Apoptosis

Annexin V assays were used to detect the early phases of apoptosis. Apoptosis was assessed by monitoring the expression of phosphatidylserine on the outer leaflet, an early marker of apoptotic cell death. Phosphatidylserine was stained with fluorescein isothiocyanate (FITC)-labeled annexin V. Loss of membrane integrity as a consequence of necrosis was detected using propidium iodide (PI) showing DNA content. Briefly, prostate cancer cells (DU145 or PC-3, 1×10^6 cells/dish) were either untreated (control) or treated with chemotherapeutic drug (rapamycin or carboplatin) or Fe_3O_4 NPs (100 μg/mL) for 48 h in the absence or presence of chemotherapeutic drug (rapamycin or carboplatin).

After incubation, cells were harvested, gently washed twice in ice-cold PBS, collected by centrifugation, and then stained using an Annexin V-FITC Kit (Beckman Coulter, Marseille, France) according to the manufacturer's instructions. Cells were then stained with Annexin V and PI for analysis by FCM within 1 h of staining using the FL1 (FITC) and FL3 (PI) lines (Beckman Coulter).

2.8. Real-Time Quantitative Polymerase Chain Reaction (RT-qPCR)

Total RNA from cells and prostate cancer tissues was extracted using ISOGEN (Nippon Gene, Toyama, Japan). cDNA was synthesized from total RNA using a High Capacity cDNA Reverse Transcription kit (Thermo Fisher Scientific, Waltham, MA, USA) with random hexamers. RT-qPCR was carried out on a fluorescent quantitative detection system (LineGene FQD-33A; Bio Flux, Tokyo, Japan). PCR was run in microtubes at a volume of 24 μL, containing 1.0 μL cDNA, 12.5 μL SYBR Premix EX Taq (Takara Bio, Shiga, Japan), 8.5 μL PCR-grade water, and 10 pmol of each pair of primers. The primers were used for the PCR as follows: 5′-CATGAGAAGTATGACAACAGCCT-3′ (forward), 5′-AGTCCTTCCACGATACCAAAGT-3′ (reverse) for glyceraldehyde 3-phosphate dehydrogenase (*GAPDH*; GenBank accession No. NM002046); 5′-AGACATGACCAGGTATGCCTAT-3′ (forward), 5′-AGCCTATCTCCTGTCGCATTA-3′ (reverse) for multiple drug resistance 1 (*MDR1*; GenBank accession No. NM000927); 5′-TATTAGAGGTCCGTGATACAGGC-3′ (forward), 5′-AGAGGGGATC ATGGAAGAGGTA-3′ (reverse) of multidrug resistance associated protein 1 (*MRP-1/ABCC1*; GenBank accession No. 019900); 5′-AACCTGGTCTCAACGCCATC-3′ (forward), 5′-GTCGCGGT GCTCCATTTATC-3′ (reverse) for breast cancer resistance protein (*BCRP/ABCG2*; GenBank accession no. NM004827). The reactions were performed for 10 s at 95 °C for preheating, then 5 s at 95 °C and 26 s at 60 °C for 40 or 45 cycles. The PCR products were subjected to subsequent agarose gel electrophoresis. The crossing point was defined as the cycle number at which the fit line in the log-linear portion of the plot intersected the threshold level. A standard curve for each gene and *GAPDH* was generated from serial dilution of the mRNA of each gene. Finally, the relative copy number was calculated as the ratio of each gene to the *GAPDH* copy number in each sample.

2.9. Western Blot Analysis

We performed western blot analysis as previously reported [12]. Cells were lysed in Radioimmunoprecipitation Assay (RIPA) buffer (Sigma-Aldrich, Tokyo, Japan) containing protease inhibitors (Sigma-Aldrich, Tokyo, Japan). The total protein concentration was determined using Bio-Rad protein assay reagents (Bio-Rad, Hercules, CA, USA). Equal amounts of lysates were resolved by sodium dodecyl sulfate-polyacrylamide gel electrophoresis and transferred to polyvinylidene fluoride membranes (Merck Millipore). Membranes were blocked with blocking reagent (NOF Corp., Tokyo, Japan) for 1 h at room temperature and incubated overnight at 4 °C with respective primary antibodies in TBST. The membranes were washed with TBST three times and incubated with diluted horseradish peroxidase (HRP)-conjugated secondary antibodies (1:3000 for nuclear factor-κB [NF-κB]; 1:10,000 for β-actin) for 1 h at room temperature. After three additional washes, the membranes were detected using an enhanced chemiluminescence (ECL) kit (GE Healthcare, Little Chalfont, UK). Antibodies against NFκB and β-actin were purchased from Santa Cruz Biotechnology (Santa Cruz Biotechnology, Santa Cruz, CA, USA) and Sigma-Aldrich, respectively; anti-rabbit and anti-mouse HRP-conjugated secondary antibodies were purchased from GE Healthcare.

2.10. Statistical Analysis

All experiments were repeated at least three times. All numeric values are presented as the mean ± standard deviation. The statistical significance of differences was determined using Student's unpaired *t*-tests. Differences between treated and untreated control cells were determined using one-way analysis of variance followed by Dunnett's test. Differences with *p* values of less than 0.05 were

considered statistically significant. The combined effect was assessed by calculating the cooperative index (CI) based on the response additivity approach [15].

$$CI = (E_A + E_B)/E_{AB}$$

where E_A and E_B are the percentage of the apoptotic fraction induced by A (Fe_3O_4 NPs) and B (rapamycin or carboplatin) alone, and E_{AB} is the percentage of the apoptotic fraction induced by the combined treatment. CI values of less than 1 indicated a synergistic effect, CI values equal to 1 indicated an additive effect, and CI values of more than 1 indicated an antagonistic effect.

3. Results

3.1. Fe₃O₄ NPs Uptake

The uptake was analyzed using FCM. After exposure of DU145 cells to Fe_3O_4 NPs, cytograms of FS and SS showed that SS increased in a concentration-dependent manner (Figure 1A). The values of FS were constant, whereas higher concentrations of Fe_3O_4 NPs resulted in higher intensities of SS (Figure 1B). These results suggested that cells taking up higher levels of Fe_3O_4 NPs showed higher intensities of SS and that uptake of Fe_3O_4 NPs occurred in a concentration-dependent manner. Upon treatment with 100 μg/mL Fe_3O_4 NPs, uptake was also detected in PC-3 (data not shown).
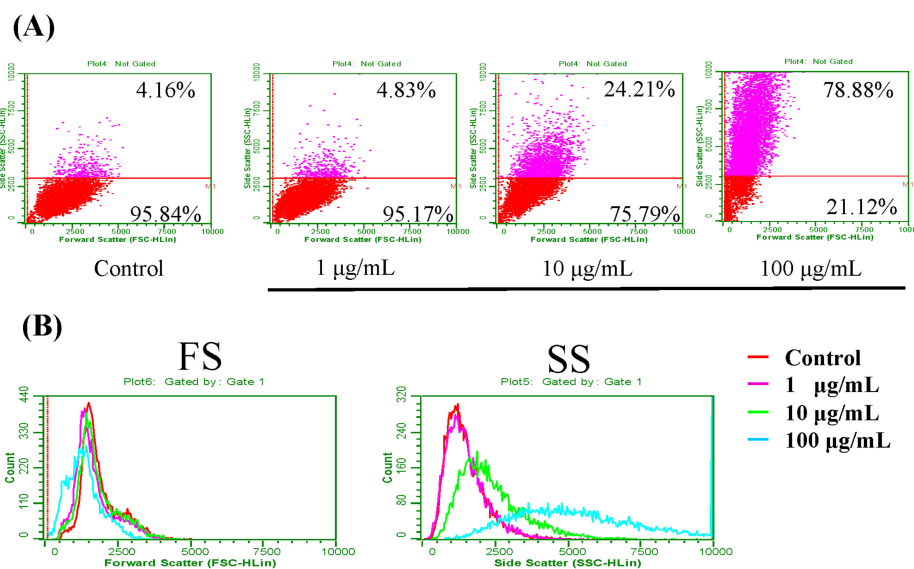

Figure 1. Analysis of Fe_3O_4 NPs uptake by Flow Cytometry (FCM). DU145 cells were treated with several concentrations of Fe_3O_4 nanoparticles (NPs) for 24 h. (**A**) FCM scatter plots of DU145 cells untreated or treated with Fe_3O_4 NPs. The vertical axis is referred to side scattering (SS), and the horizontal axis referred to the forward scattering (FS); (**B**) FCM histograms of FS and SS. Concentration-dependent comparison of FS and SS intensity.

3.2. Effects of Fe₃O₄ NPs on Cell Viability

Each cell line was treated with 1, 10, or 100 μg/mL Fe_3O_4 NPs for 24 or 72 h (Figure 2). The viability of DU145 cells was reduced significantly after treatment with 100 μg/mL Fe_3O_4 NPs for 72 h ($p < 0.01$, 91.1 ± 3.4), and the viability of PC-3 cells was reduced significantly at after treatment with 10 and 100 μg/mL Fe_3O_4 NPs for 24 h ($p < 0.01$, 91.7 ± 3.9 and 90.1 ± 4.3, respectively) and 72 h ($p < 0.01$, 89.8 ± 4.4 and 86.4 ± 4.4, respectively). Differences in inhibitory effects were detected for both cell lines, showing that PC-3 cells were more sensitive to Fe_3O_4 NPs than DU145 cells.
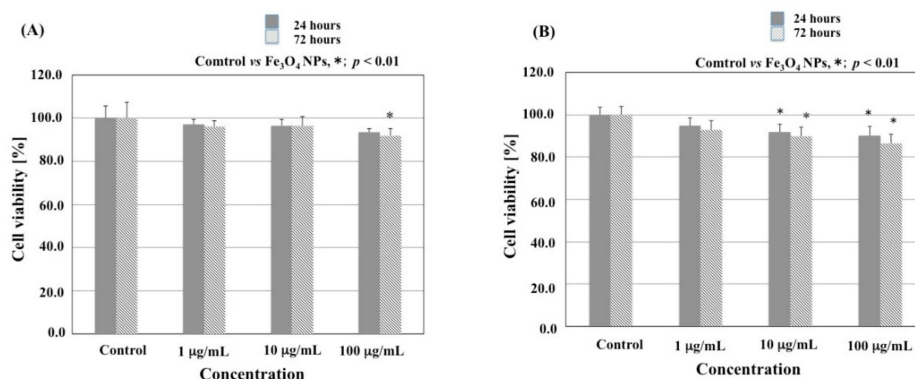
Figure 2. Effects of Fe_3O_4 NPs on cell viability. (**A**) DU145 cells were treated with several concentrations of Fe_3O_4 NPs for 24 and 72 h; (**B**) PC-3 cells were treated with several concentrations of Fe_3O_4 NPs for 24 and 72 h. * Significantly different from the untreated control at $p < 0.01$.

3.3. ROS Production in Cells Treated with Fe_3O_4 NPs

CM-H_2DCFDA (Invitrogen, Carlsbad, CA, USA) assays were used to assess the impact of Fe_3O_4 NPs on cellular ROS production in DU145 and PC-3 cells. DU145 and PC-3 cells treated with Fe_3O_4 NPs showed a concentration-dependent ROS production compared with both cells without Fe_3O_4 NPs; significant increases were observed at 10 and 100 µg/mL after 24 h in both cell lines ($p < 0.01$; Figure 3). ROS production in PC-3 cells was higher than that in DU145 cells ($p < 0.01$ at 10 µg/mL, and $p < 0.05$ at 100 µg/mL), similar to our previous data (Figure 3). ROS production in both cell lines was similar after treatment with 100 µg/mL Fe_3O_4 NPs or treatment with H_2O_2.
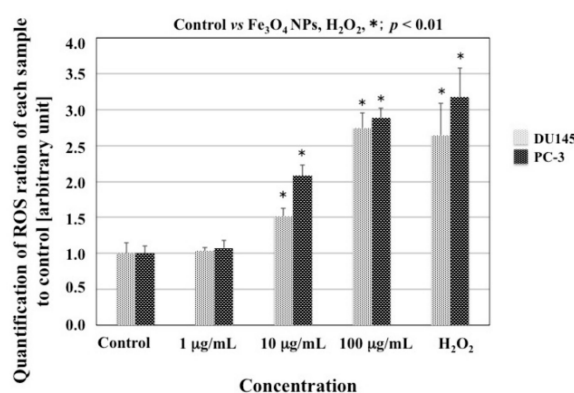

Figure 3. Production of intracellular reactive oxygen species (ROS) at 24 h after treatment with Fe_3O_4 NPs. * Significantly different from the untreated control at $p < 0.01$.

3.4. Effects of Fe_3O_4 NPs on the Cell Cycle

The effects of Fe_3O_4 NPs on cell cycle progression and population distribution in DU145 and PC-3 cells were analyzed by FCM (Table 1). The results showed a slight increase in the percentage of the cell population in G_0/G_1 phase in PC-3 cells and a slight decrease in the percentage of the cell population in G_0/G_1 phase in DU145 cells after treatment with 100 µg/mL Fe_3O_4 NPs alone. However, there were no significant differences between Fe_3O_4 NPs and control treatments.

Table 1. Effect of Fe_3O_4 NPs on cell cycle of prostate cancer cells.

PC-3	Sub-G_1	G_0/G_1	S	G_2
Control	3.3 ± 0.1	66.1 ± 0.3	8.0 ± 0.2	22.7 ± 0.3
Fe_3O_4 NPs (1 g/mL)	4.5 ± 0.2	68.2 ± 0.5	8.3 ± 0.1	19.0 ± 0.7
Fe_3O_4 NPs (10 g/mL)	5.1 ± 0.2	67.9 ± 0.5	8.4 ± 0.1	18.5 ± 0.6
Fe_3O_4 NPs (100 g/mL)	5.5 ± 0.1	68.7 ± 0.3	8.9 ± 0.2	16.9 ± 0.3
DU145	**Sub-G_1**	**G_0/G_1**	**S**	**G_2**
Control	0.5 ± 0.1	53.7 ± 0.3	5.1 ± 0.1	40.8 ± 0.4
Fe_3O_4 NPs (1 g/mL)	0.5 ± 0.1	52.3 ± 0.4	5.7 ± 0.1	41.4 ± 0.4
Fe_3O_4 NPs (10 g/mL)	0.5 ± 0.1	53.0 ± 0.2	5.8 ± 0.1	40.8 ± 0.3
Fe_3O_4 NPs (100 g/mL)	0.6 ± 0.1	50.9 ± 0.7	8.5 ± 0.4	40.0 ± 1.1

3.5. Combined Effects of Fe_3O_4 NPs and Chemotherapeutic Agents on Cell Viability

Next, we investigated the inhibitory effects of treatment with rapamycin or carboplatin alone or with each chemical agent combined with Fe_3O_4 NPs on prostate cancer cell growth using alamarBlue assays. Treatment with rapamycin induced a concentration-dependent decrease in viability in both cell lines ($p < 0.01$ at 1, 10 and 20 nM in PC-3 cells; $p < 0.05$ at 1 nM, $p < 0.01$ at 10 and 20 nM in DU145 cells; Figure 4A). Treatment with carboplatin also induced a concentration-dependent decrease in viability in both cell lines ($p < 0.01$ at 10, 20 and 30 μM; Figure 4B). The selection of the dose for chemotherapeutic agents was based on a dose-seeking study showing approximately 25% inhibition in cell growth (Figure 4A,B). Interestingly, Alamar Blue assays showed that 10 nM rapamycin combined with Fe_3O_4 NPs induced a concentration-dependent decrease in viability in DU145 cells ($p < 0.01$ at 1, 10, and 100 μg/mL Fe_3O_4 NPs) and in PC-3 cells ($p < 0.01$; 100 μg/mL Fe_3O_4 NPs; Figure 4C). Moreover, Alamar Blue assays showed that 10 μM carboplatin combined with Fe_3O_4 NPs produced a concentration-dependent reduction in cell viability in DU145 cells ($p < 0.05$ at 10 μg/mL, and $p < 0.01$ at 100 μg/mL Fe_3O_4 NPs) and in PC-3 cells at 100 μg/mL Fe_3O_4 NPs ($p < 0.01$; Figure 4D).
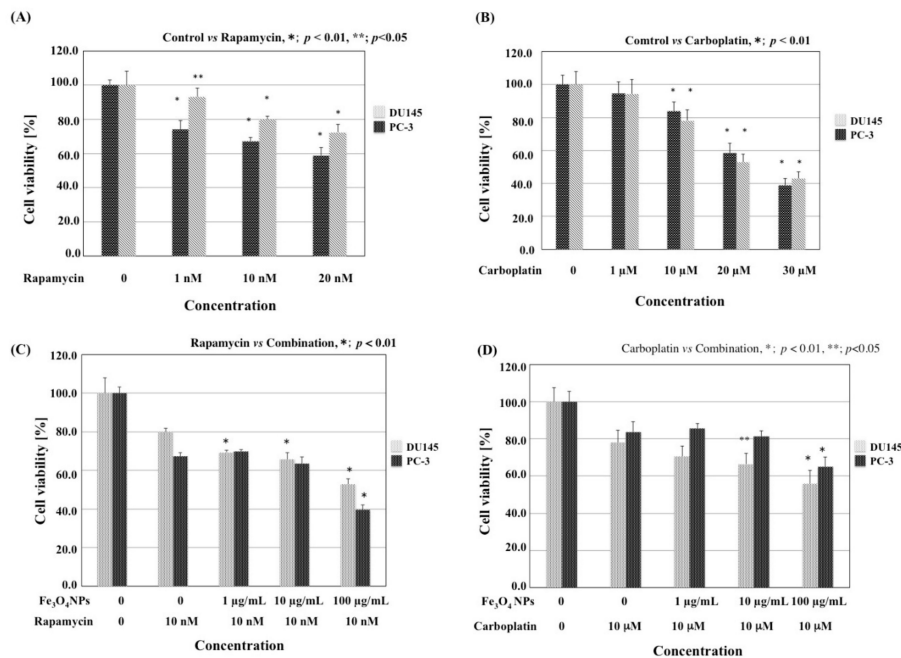

Figure 4. Effects of chemotherapeutic agents alone and in combination with Fe_3O_4 NPs on cell viability. (**A**) Effects of rapamycin on PC-3 or DU145 cell viability for 24 h; (**B**) Effects of carboplatin on PC-3 or DU145 cell viability for 24 h; (**C**) DU145 or PC-3 cells were treated with rapamycin alone or in combination for 24 h; and (**D**) DU145 or PC-3 cells were treated with carboplatin alone or in combination for 24 h. * Significantly different from the group with chemotherapeutic agent alone at $p < 0.01$; ** significantly different from the group with chemotherapeutic agent alone at $p < 0.05$.

3.6. Combined Effects of Fe₃O₄ NPs and Chemotherapeutic Agents on Apoptosis

To determine the effects of combined Fe₃O₄ NPs and rapamycin/carboplatin, we chose to treat prostate cancer cells with 100 μg/mL Fe₃O₄ NPs and 10 nM rapamycin or 100 μg/mL Fe₃O₄ NPs and 10 μM carboplatin. FCM analysis showed a strong induction of apoptosis by the combination of 100 μg/mL Fe₃O₄ NPs and 10 nM rapamycin in PC-3 cells (Figure 5A). The portions of Annexin V(+)/PI(−) and Annexin V(+)/PI(+) cells indicated the early and late stages of apoptosis. The quantitative data showed that the effects varied with cell type and chemotherapeutic agent (Figure 5B–E). Their combinations (ramamycin and Fe₃O₄ NPs in PC-3 cells, and carboplatin and Fe₃O₄ NPs in DU145 cells) resulted in a significant increase in apoptotic cells compared to each chemotherapeutic drug alone ($p < 0.01$ and $p < 0.05$, respectively). In addition, to determine whether the effects of the combined treatment were synergistic, the CI was calculated based on the response additivity approach. When PC-3 cells were treated with Fe₃O₄ NPs together with rapamycin or carboplatin, the CIs were 0.97 (Figure 5B) and 1.36 (Figure 5D), respectively; additionally, when DU145 cells were treated with Fe₃O₄ NPs together with rapamycin or carboplatin, the CIs were 1.20 (Figure 5C) and 0.93 (Figure 5E), respectively. Synergistic effects were observed in PC-3 cells treated with Fe₃O₄ NPs and rapamycin (Figure 5B) and in DU145 cells treated with Fe₃O₄ NPs and carboplatin (Figure 5E).
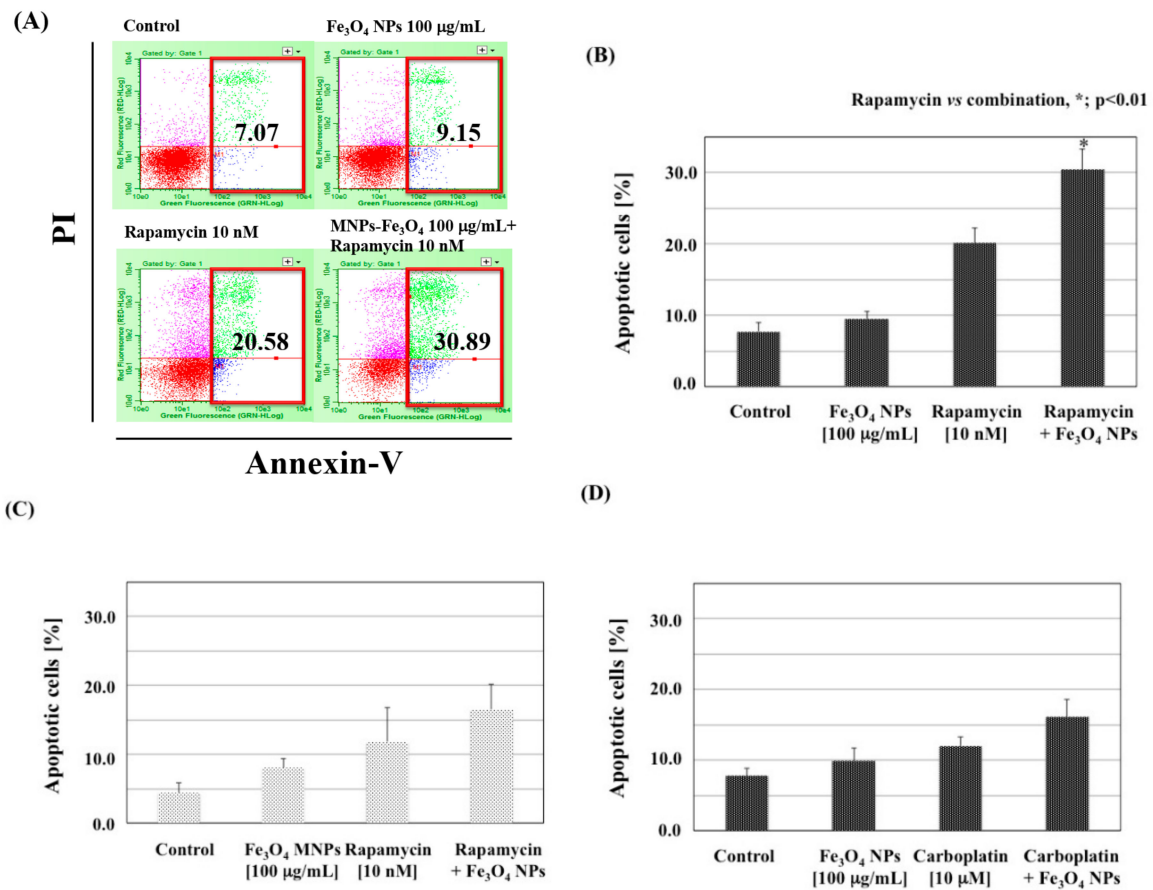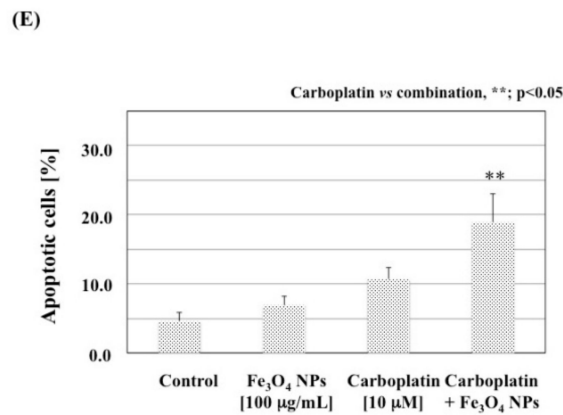

Figure 5. *Cont.*

(E)

Figure 5. Combined effect of Fe₃O₄ NPs and chemotherapeutic agents on apoptosis. DU145 or PC-3 cells were treated with Fe₃O₄ NPs, carboplatin, rapamycin or their combinations for 48 h. Cells were then harvested, stained with Annexin V and PI, and analyzed by FCM. (**A**) Representative case of FCM in PC3 cells. The portions surrounded by the line mean the early and late stages of apoptosis; (**B**) Comparison of apoptotic rates among PC-3 cells treated with Fe₃O₄ NPs, rapamycin alone, or combination treatment; (**C**) Comparison of apoptotic rates among DU145 cells treated with Fe₃O₄ NPs, rapamycin alone, or combination treatment; (**D**) Comparison of apoptotic rates among PC-3 cells treated with Fe₃O₄ NPs, carboplatin alone, or combination treatment; (**E**) Comparison of apoptotic rates among DU145 cells treated with Fe₃O₄ NPs, carboplatin alone, or combination treatment. * Significantly different from the group with chemotherapeutic agent alone at $p < 0.01$; ** significantly different from the group with chemotherapeutic agent alone at $p < 0.05$.

3.7. Effects of Fe₃O₄ NPs, Chemotherapeutic Agents, and Their Combinations on the Expression of MDR1, MRP1, and BCRP mRNA in Prostate Cancer Cells

To determine whether the development of chemosensitivity in both cell lines was associated with decreased expression of ABC transporter genes, we examined the expression of *MDR1*, *ABCC1*, and *ABCG2* mRNAs (Figure 6). *MDR1* expression was not detected in both cell lines (data not shown). In both cells treated with MNPs and carboplatin/rapamycin, *ABCC1* and *ABCG2* levels were altered; however, these differences were not significant.
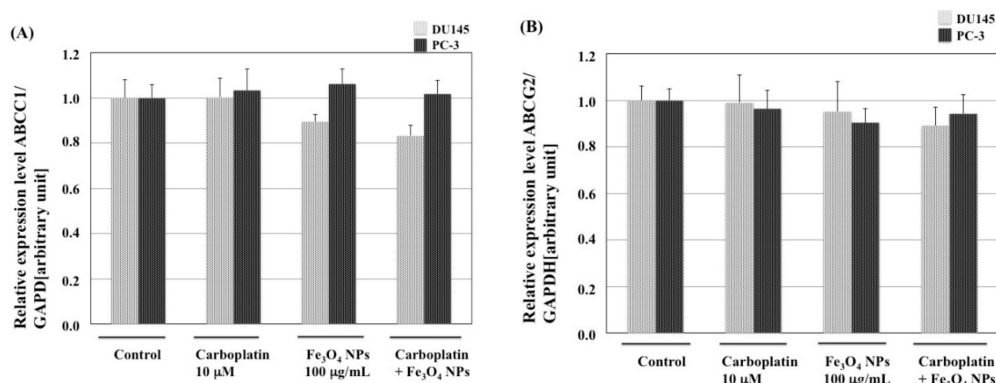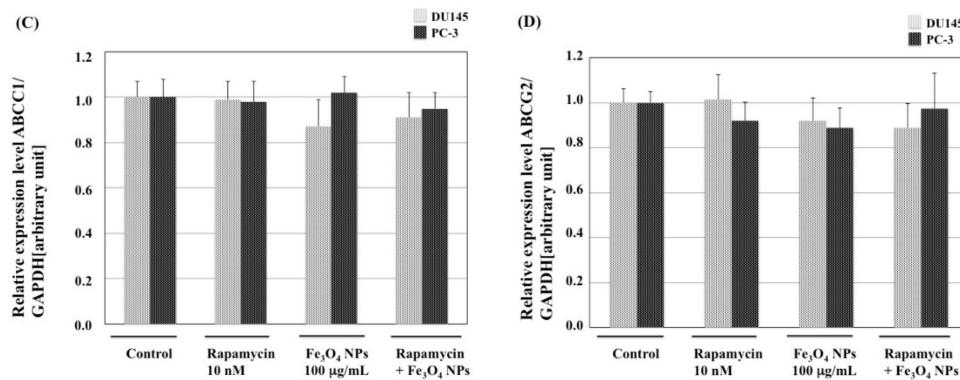

Figure 6. *Cont.*

Figure 6. Expression of ABC (ATP-binding cassette) transporter mRNAs in prostate cancer cells. (**A**) ABCC1 (ATP-binding cassette subfamily C member 1) mRNA expression in prostate cancer cells untreated, and treated with carboplatin, MNPs, or combination treatment; (**B**) ABCG2 (ATP-binding cassette subfamily G member 2) mRNA expression in prostate cancer cells untreated, and treated with carboplatin, MNPs, or combination treatment; (**C**) ABCC1 mRNA expression in prostate cancer cells untreated, and treated with rapamycin, Fe_3O_4 NPs, or combination treatment; (**D**) ABCG2 mRNA expression in prostate cancer cells untreated, and treated with rapamycin, Fe_3O_4 NPs, or combination treatment.

3.8. Effects of Fe_3O_4 NPs, Chemotherapeutic Agents, and Their Combinations on NF-κB Expression in Prostate Cancer Cells

The effects of Fe_3O_4 NPs, rapamycin, and carboplatin alone or in combination on NF-κB expression in both cell lines were analyzed. Combination treatment of Fe_3O_4 NPs with rapamycin in PC-3 cells and with carboplatin in DU145 cells tended to decrease NF-κB expression, although the difference was not significant (Figure 7).
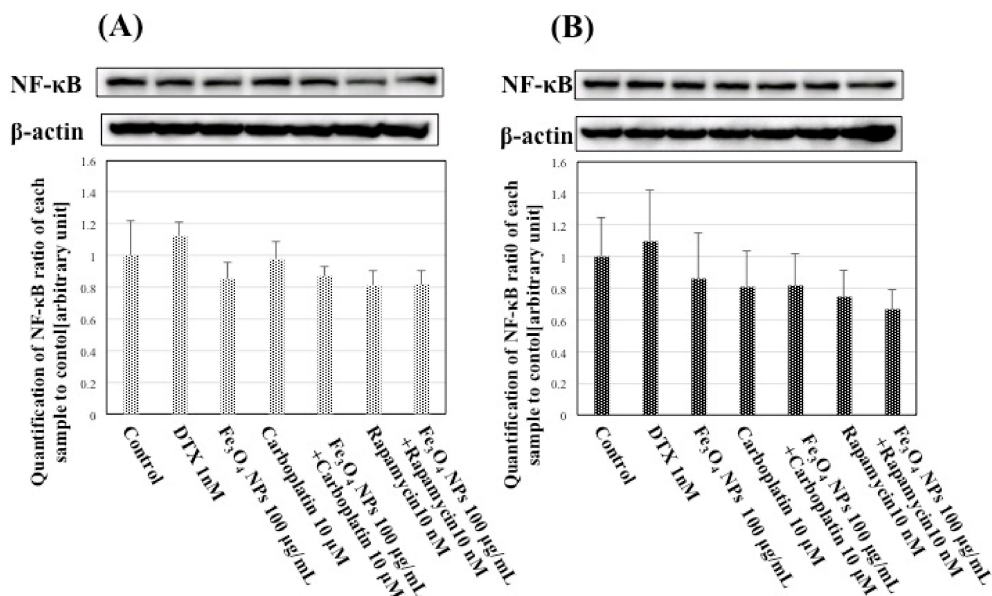

Figure 7. Western blot analysis of the expression levels of NF-κB in prostate cancer cells. (**A**) Effects of Fe_3O_4 NPs, rapamaycin, carboplatin alone, or combination treatment on NF-κB expression in DU145 cells; (**B**) Effects of Fe_3O_4 NPs, rapamaycin, carboplatin alone, or combination treatment on NF-κB expression in PC-3 cells. DTX was used because NF-κB signal pathway was activated by DTX [16].

4. Discussion

The development of NP has facilite the establishment of potential treatments for malignancy because of the ability to selectively deliver chemotherapeutic agents to malignant cells, control release, and minimize off-target toxicity. Notably, the effects of NPs, such as iron oxide, selenium, silver, and gold NPs, alone or with different therapies (e.g., chemical agents or photocatalytic therapy) on malignant cells have been also reported [17–21]. These therapies are mainly based on interactions with malignant cells via the generation of ROS [22]. In the present study, we examined the effect of Fe_3O_4 NPs combined with rapamycin or carboplatin on prostate cancer cell growth in vitro in order to explore the possible applications of Fe_3O_4 NPs for modification of chemotherapeutic agent usage in patients with CRPC.

In this study, to uptake Fe_3O_4 NPs in DU145 and PC-3 cells was analyzed using FCM. The uptake of Fe_3O_4 NPs by both cells was recognized in a dose-dependent manner as we have previously shown cellular uptake of MNPs-Fe_3O_4 in prostate cancer cells by TEM [12]. The physicochemical properties of the NPs including size, shape, and surface charge have various effects on their interactions with living cells such as cellular uptake, localization and cytotoxicity [23]. Small NPs have a high probability to be internalized by passive uptake than large one. In addition, culture media with/without FBS have been reported to affect the size stability in vitro systems, showing that NPs aggregated in a high-ionic-strength medium such as PBS or RPMI-1640 solution because of the suppression of the double layer, which reduces the electrostatic repulsion barrier [24,25]. In this study, aggregation of Fe_3O_4 NPs was observed in culture media, and induced ROS production in a dose-dependent manner. Thus, this is an interesting, leading that complex of MNPs, a chemotherapeutic agent and FBS may effect on interactions such as cellular uptake via alternative endocytosis pathways [26]. However, there remains a problem to be solved by further studies.

In this study, ROS production in DU145 and PC-3 cells after exposure to Fe_3O_4 NPs was observed in a dose-dependent manner, similar to our previous findings [12]. Thus, we predicted that Fe_3O_4 NPs may enhance rapamycin- or carboplatin-induced prostate cancer cell death in both cell lines, similar to that in combination treatment with DTX. Fe_3O_4 NPs have been reported to cause low toxicity or cytotoxicity at concentrations of 100 μg/mL or higher via the generation of ROS, which can result in lipid peroxidation, DNA damage, and protein oxidation [27]. ROS, resulting from the transfer of energy or electrons to oxygen, act as a second messenger in cell signaling and are involved in various biological processes, including growth and survival in normal cells. Their levels in cells are controlled by enzymes such as superoxide dismutase, glutathione peroxidase, and catalase, as well as antioxidants. Oxidative stress results from an imbalance between ROS generation and elimination. The high ROS levels in cancer cells, which are a consequence of alterations in several signaling pathways, play important roles in initiation, progression, and metastasis; thus, ROS are considered oncogenic [28,29]. However, because ROS are also implicated in triggering cell death, including that of cancer cells, their production is desirable in chemotherapy, radiotherapy, and photodynamic therapy [22]. Notably, oxidative stress has been shown to have a prominent role in the pathogenesis of prostate cancer [28]. In particular, oxidative stress is involved in the conversion of androgen-dependent prostate cancer into CRPC via regulation of androgen receptor expression [29]. Excessive accumulation of ROS may tip over a threshold, leading to cell toxicity, making some tumor cells susceptible to ROS-induced apoptosis. A differential response between tumor and normal cells has been reported in some studies involving prostate cancer cells, supporting the design of new strategies in prostate cancer therapy [30]. In our previous report, Fe_3O_4 NPs was found to enhance DTX-induced prostate cancer cell death, and ROS levels were found to increase with exposure, similar to the levels of 8-OH-dG, a marker of oxidative DNA damage with exposure in DU145 and PC-3 cells [12]. A slight difference of cell viability between DU145 and PC-3 was observed in this study although both cell lines showed to increase ROS production as same as the previous study [12]. In addition, Fe_3O_4 NPs alone reduced the viability of LNCaP and PC-3 cells, but had little or no effect on the viability of DU145 and PrSC cells [12]. PrSC cells were prostate stromal cells, and used as normal control. These results suggest

that the cytotoxicity of Fe_3O_4 NPs may be dependent on the cell type, which may be linked with the different redox state properties.

Multiple pathways, including apoptosis, inflammation, and drug efflux pumps, are implicated in chemoresistance of prostate cancer [31]. The expression of NF-κB, a transcriptional factor for survival signaling pathways, increases in DU145 cells treated with DTX [16]. Fe_3O_4 NPs were also found to enhance the inhibitory effects of DTX via suppression of NF-κB expression [12]. However, significant suppression of NF-κB expression was not observed in prostate cancer cell lines treated with a combination of Fe_3O_4 NPs and rapamycin or carboplatin. In addition, ROS has been reported to up- or down-regulate the expression of p-glycoprotein in various cells [32–34]. Recently, AgNP treatment has also been reported to inhibit the efflux activity of drug-resistant cells [20]. The authors mentioned that it was necessary to clarify whether AgNPs exerted their inhibitory effects directly on the ABC transporter itself, through disruption of mitochondrial function and ATP production, or by transcriptional silencing of the *mdr1*-encoding genomic locus [20]. These findings suggest that NPs may have the potential to affect the expressions of ABC transporters in cells via various pathways. However, in this study, significant suppression of *ABCC1* and *ABCG1* expression was not observed in either cell line following combined treatment with Fe_3O_4 NPs and rapamycin or carboplatin. Additional experiments are needed to clarify the mechanisms through which the effects of chemotherapies are enhanced by the combination treatment.

In this study, we found that the characteristics of different cell lines may play a key role in determining the effects of Fe_3O_4 NPs combined with rapamycin or carboplatin. The phosphatidylinositol 3-kinase (PI3K)/Akt/mTOR pathway is a key signaling pathway in prostate cancer progression [35]. Rapamycin and its analogs (rapalogs) were the first identified inhibitors of the PI3K/Akt/mTOR pathway and were found to inhibit tumor growth in mouse xenograft models derived from $PTEN^{-/-}$ PC-3 and $PTEN^{+/-}$ DU145 cells [36]. However, rapamycin and rapalogs did not show clinical benefits as single agents because they did not inhibit mTOR complex 2 (mTORC2), which activates Akt in prostate cancer cells. In this study, Fe_3O_4 NPs enhanced the inhibitory effects of rapamycin in both prostate cancer cell lines, and combination of Fe_3O_4 NPs with other chemotherapeutic agents was more effective in PC-3 cells when a concentration of 100 μg/mL Fe_3O_4 NPs was used. In addition, combined treatment with Fe_3O_4 NPs and rapamycin in PC-3 cells synergistically enhanced induction of apoptosis. Fe_3O_4 NPs have been reported to induce AKT activation, demonstrating that this pathway is involved in cellular proliferation after exposure of Fe_3O_4 NPs. Moreover, increased oxidative stress in melanoma cells has been shown to inhibit the PI3K/Akt/mTOR pathway through mTORC1 formation and phosphorylation of downstream targets [37]. Although intracellular molecular mechanisms are complex, these results indicate that this combination may represent a new therapeutic option via acute ROS formation; the involvement of mTORC1 and/or mTORC2 inhibition in this process requires further clarification.

Platinum drugs exert their biological activity via reactive biotransformation products that bind to DNA; this results in the formation of DNA adducts that inhibit DNA replication, induce cell cycle arrest, and promote apoptosis. Carboplatin is a second-generation platinum agent that has fewer serious side effects than cisplatin. At present, none of the treatment regimens have demonstrated a significant overall survival benefit [38]. However, these platinum drugs are expected to be useful for a specific subtype of patients with HRPC, particularly in certain histological types such as neuroendocrine carcinoma. In this study, combination of Fe_3O_4 NPs with carboplatin also decreased the viability of DU145 and PC-3 cells compared with carboplatin alone. Moreover, combined treatment with Fe_3O_4 NPs and carboplatin in DU145 cells synergistically enhanced induction of apoptosis. ROS production may modulate this enhancement of carboplatin effects by Fe_3O_4 NPs because platinum drugs have been reported to induce mitochondrion-dependent ROS production, which significantly contributes to cell killing by enhancing the cytotoxic effects exerted through the formation of DNA damage [39].

These drugs have been referred to as "old drugs". If they have substantial toxicity, the risk-benefit ratio may be positive by predicting sensitivity to the combination of old drugs and iron oxide NPs based on the genetic background (e.g., PTEN and p53).

The use of MNPs in chemotherapy, gene therapy, hyperthermia, photochemical ablation, and photodynamic therapy has been proposed [19]. Encapsulating or attaching molecular drugs to iron oxide NPs helps selectively deliver chemotherapeutics to target cells, allows for decreased dosage, and minimizes off-target toxicity. In addition, the combination of hyperthermia and chemotherapy in the same MNPs-based nanotherapeutic system is relatively new. Enhancement of the effects of chemotherapy with application of concurrent hyperthermia is called thermo-chemosensitization, which is dependent on the synergistic effects of hyperthermia and chemotherapy [40]. The thermal enhancement of drug cytotoxicity is maximized at mild hyperthermia temperatures and does not require temperature as high as those used for hyperthermia therapy alone.

5. Conclusions

In summary, in this study, we found that treatment with a combination of Fe_3O_4 NPs and low doses of rapamycin or carboplatin inhibited prostate cancer cell growth in vitro via ROS production, with cell line-dependent effects. These findings showed the possibility that the combination of Fe_3O_4 NPs with low doses of various chemotherapeutic agents could be a novel therapeutic strategy for patients with CRPC.

Author Contributions: Kanako Kojima conceived, designed the experiments mainly, performed Western blot analysis and wrote the paper partially, Sanai Takahashi performed RT-qPCR, Shungo Saito and Yoshihiro Endo, performed FCM analysis for cell cycle and apoptosis, Tadashi Nittami performed cell culture, Tadashige Nozaki helped analysis of the data, Masatoshi Watanabe supervised the project and wrote the paper. The idea originated from the discussion between Masatoshi Watanabe and Ranbir Chander Sobti.

Conflicts of Interest: The authors declare no conflict of interest. The founding sponsors had no role in the design of this study.

Abbreviations

ADT	Androgen-deprivation therapy
ABCC1	ATP-binding cassette subfamily C member 1
ABCG2	ATP-binding cassette subfamily G member2
BCRP	Breast Cancer Resistance Protein
CRPC	Castration-Resistant Prostate Cancer
CI	Cooperative Index
DMSO	Dimetyl sulfoxide
DTX	Docetaxel
DLS	Dynamic light scattering
FBS	Fetal bovine serum
Fe_3O_4 NPs	Fe_3O_4 nanoparticles
FCM	Flow cytometry
FITC	Fluorescein isothiocyanate
FS	Forward-scattered
GAPDH	Glyceraldehyde 3-phosphate dehydrogenase
MNPs	Magnetic nanoparticles
mTOR	mammalian target of rapamycin
mCRPC	metastatic castration-resistant prostate cancer
MRP1	Multiple drug resistance 1
NPs	Nanoparticles
NF-κB	Nuclear Factor-kappa B
PBS	phosphate-buffered saline

PDI   Polydispersity index
PI   Propidium Iodide
PSA   Prostate-Specific Antigen
ROS   Reactive Oxygen Species
RT-qPCR   Real-time quantitateive polymerase chain reaction
SS   Side-scattered
TEM   Transmission electron microscopy
XRD   X-ray powder diffraction

References

1. Siegel, R.L.; Miller, K.D.; Jemal, A. Cancer statistics, 2016. *CA Cancer J. Clin.* **2016**, *66*, 7–30. [CrossRef] [PubMed]

2. Seisen, T.; Rouprêt, M.; Gomez, F.; Malouf, G.G.; Shariat, S.F.; Peyronnet, B.; Spano, J.P.; Cancel-Tassin, G.; Cussenot, O. A comprehensive review of genomic landscape, biomarkers and treatment sequencing in castration-resistant prostate cancer. *Cancer Treat. Rev.* **2016**, *48*, 25–33. [CrossRef] [PubMed]

3. Chandrasekar, T.; Yang, J.C.; Gao, A.C.; Evans, C.P. Mechanisms of the resistance in castration-resistance prostate cancer (CRPC). *Transl. Androl. Urol.* **2015**, *4*, 365–380. [PubMed]

4. Chakraborty, M.; Jain, S.; Rani, V. Nanotechnology: Emerging tool for diagnostic and therapeutics. *Appl. Biochem. Biotechnol.* **2011**, *165*, 1178–1187. [CrossRef] [PubMed]

5. Mahmoudi, M.; Sant, S.; Wang, B.; Laurent, S.; Sen, T. Superparamagnetic iron oxide nanoparticles (SPIONs): Development, surface modification and applications in chemotherapy. *Adv. Drug Deliv. Rev.* **2011**, *63*, 24–46. [CrossRef] [PubMed]

6. Vinardell, M.P.; Mitjans, M. Antitumor activities of metal oxide nanoparticles. *Nanomaterials* **2015**, *5*, 1004–1021. [CrossRef] [PubMed]

7. Calero, M.; Chiappi, M.; Lazaro-Carrillo, A.; Rodríguez, M.J.; Chichón, F.J.; Crosbie-Staunton, K.; Prina-Mello, A.; Volkov, Y.; Villanueva, A.; Carrascosa, J.L. Characterization of interaction of magnetic nanoparticles with breast cancer cells. *J. Nanotechnol.* **2015**, *13*, 16. [CrossRef] [PubMed]

8. Chen, B.A.; Dai, Y.; Wang, X.M.; Zhang, R.Y.; Xu, W.L.; Shen, H.L.; Gao, F.; Sun, Q.; Deng, X.J.; Ding, J.H.; et al. Synergistic effect of the combination of nanoparticulate Fe_3O_4 and Au with daunomycin on K562/A02 cells. *Int. J. Nanomed.* **2008**, *3*, 343–350. [CrossRef]

9. Chen, B.; Cheng, J.; Shen, M.; Gao, F.; Xu, W.; Shen, H.; Ding, J.; Gao, C.; Sun, Q.; Sun, X.; et al. Magnetic nanoparticle of Fe_3O_4 and 5-bromotetrandrin interact synergistically to induce apoptosis by daunorubicin in leukemia cells. *Int. J. Nanomed.* **2009**, *4*, 65–71.

10. Jing, H.; Wang, J.; Yang, P.; Ke, X.; Xia, G.; Chen, B. Magnetic Fe_3O_4 nanoparticles and chemotherapy agents interact synergistically to induce apoptosis in lymphoma cells. *Int. J. Nanomed.* **2010**, *5*, 999–1004.

11. Zhang, W.; Qiao, L.; Wang, X.; Senthilkumar, R.; Wang, F.; Chen, B. Inducing cell cycle arrest and apoptosis by dimercaptosuccinic acid modified Fe_3O_4 magnetic nanoparticles combined with nontoxic concentration of bortezomib and gambogic acid in RPMI-8226 cells. *Int. J. Nanomed.* **2015**, *10*, 3275–3289.

12. Sato, A.; Itcho, N.; Ishiguro, H.; Okamoto, D.; Kobayashi, N.; Kawai, K.; Kasai, H.; Kurioka, D.; Uemura, H.; Kubota, Y.; et al. Magnetic nanoparticles of Fe_3O_4 enhance docetaxel-induced prostate cancer cell death. *Int. J. Nanomed.* **2013**, *8*, 3151–3160.

13. Suzuki, H.; Toyooka, T.; Ibuki, Y. Simple and easy method to evaluate uptake potential of nanoparticles in mammalian cells using a flow cytometric light scatter analysis. *Environ. Sci. Technol.* **2007**, *41*, 3018–3024. [CrossRef] [PubMed]

14. Zucker, R.M.; Massaro, E.J.; Sanders, K.M.; Degn, L.L.; Boyes, W.K. Detection of TiO_2 nanoparticles in cells by flow cytometry. *Cytom. Part A* **2010**, *77*, 677–685. [CrossRef] [PubMed]

15. Foucquier, J.; Guedj, M. Analysis of drug combinations: Current methodical landscape. *Pharmacol. Res. Perspect.* **2015**, *3*, e00149. [CrossRef] [PubMed]

16. Codony-Servat, J.; Marin-Aguilera, M.; Visa, L.; García-Albéniz, X.; Pineda, E.; Fernández, P.L.; Filella, X.; Gascón, P.; Mellado, B. Nuclear factor-kappa B and interleukin-6 related docetaxel resistance in castration-resistant prostate cancer. *Prostate* **2013**, *73*, 512–521. [CrossRef] [PubMed]

17. Gao, F.; Yuan, Q.; Gao, L.; Cai, P.; Zhu, H.; Liu, R.; Wang, Y.; Wei, Y.; Huang, G.; Liang, J.; et al. Cytotoxicity and therapeutic effect of irinotecan combined with selenium nanoparticles. *Biomaterials* **2014**, *35*, 8854–8866. [CrossRef] [PubMed]

18. Xiong, X.; Arvizo, R.A.; Saha, S.; Robertson, D.J.; McMeekin, S.; Bhattachrya, R.; Mukherjee, P. Sensitization of ovarian cancer cells to cisplatin by gold nanoparticles. *Oncotarget* **2014**, *5*, 6453–6465. [CrossRef] [PubMed]

19. Gobbo, O.L.; Sjaastad, K.; Radomski, M.W.; Volkov, Y.; Prina-Mello, A. Magnetic nanoparticles in cancer theranostics. *Theranostics* **2015**, *5*, 1249–1263. [CrossRef] [PubMed]

20. Kovács, D.; Szőke, K.; Igaz, N.; Spengler, G.; Molnár, J.; Tóth, T.; Madarász, D.; Rázga, Z.; Kónya, Z.; Boros, I.M.; et al. Silver nanoparticles modulate ABC transporter activity and enhance chemotherapy in multidrug resistant cancer. *Nanomedicine* **2016**, *12*, 601–610. [CrossRef] [PubMed]

21. Petrushev, B.; Boca, S.; Simon, T.; Berce, C.; Frinc, I.; Dima, D.; Selicean, S.; Gafencu, G.A.; Tanase, A.; Zdrenghea, M.; et al. Gold nanoparticles enhance the effect of tyrosine kinase inhibitors in acute myeloid leukemia therapy. *Int. J. Nanomed.* **2016**, *11*, 641–660.

22. Wang, J.; Yi, J. Cancer cell killing via ROS: To increase or decrease, that is the question. *Cancer Biol. Ther.* **2008**, *7*, 1875–1884. [CrossRef] [PubMed]

23. Shang, L.; Nienhaus, K.; Nienhaus, G.U. Engineered nanoparticles interacting with cells: Size matters. *J. Nanobiotechnol.* **2014**, *12*, 5. [CrossRef] [PubMed]

24. Wiogo, H.T.R.; Lim, M.; Bulmus, V.; Yun, J.; Aml, R. Stabilization of magnetic iron oxide nanoparticles in biological media by fetal bovine serum (FBS). *Langmuir* **2011**, *27*, 843–850. [CrossRef] [PubMed]

25. Sabuncu, A.C.; Grubbs, J.; Qian, S.; Abdel-Fattah, T.M.; Stacey, M.W.; Beskok, A. Probing nanoparticle interactions in cell culture media. *Colloids Surf. B Biointerfaces* **2012**, *95*, 96–102. [CrossRef] [PubMed]

26. Moore, T.L.; Rodriguez-Lorenzo, L.; Hirsch, V.; Balog, S.; Urban, D.; Jud, C.; Rothen-Rutishauser, N.; Lattuada, M.; Petri-Fink, A. Nanoparticl coolidal stability in cell culture media and impact on cellular interactions. *Chem. Soc. Rev.* **2015**, *44*, 6287–6305.

27. Singh, N.; Jenkins, G.J.S.; Asadi, R.; Doak, S.H. Potential toxicity of superparamagnetic iron oxide nanoparticles (SPION). *Nano Rev.* **2010**, *1*, 10. [CrossRef] [PubMed]

28. Khandrika, L.; Kumar, B.; Koul, S.; Maroni, P.; Koul, H.K. Oxidative stress in prostate cancer. *Cancer Lett.* **2009**, *282*, 125–136. [CrossRef] [PubMed]

29. Shiota, M.; Yokomizo, A.; Naito, S. Oxidative stress and androgen receptor signaling in the development and progression of castration-resistant prostate cancer. *Free Radic. Biol. Med.* **2011**, *51*, 1320–1328. [CrossRef] [PubMed]

30. Chaiswing, L.; Zhong, W.; Oberley, T.D. Distinct redox profiles of selected human prostate carcinoma cell lines: Implications of radiational design of redox therapy. *Cancers* **2011**, *3*, 3557–3584. [CrossRef] [PubMed]

31. Mahon, K.L.; Henshall, S.M.; Sutherland, R.L.; Horvath, L.G. Pathways of chemotherapy resistance in castration-resistant prostate cancer. *Endocr. Relat. Cancer* **2011**, *18*, R103–R123. [CrossRef] [PubMed]

32. Wartenberg, M.; Hoffmann, E.; Schwaindt, H.; Grünheck, F.; Petros, J.; Arnold, J.R.; Hescheler, J.; Sauer, H. Reactive oxygen species-linked regulation of the multidrug resistance transporter P-glycoprotein in Nox-1 overexpressing prostate tumor spheroids. *FEBS Lett.* **2005**, *579*, 4541–4549. [CrossRef] [PubMed]

33. Chen, J.; Ding, Z.; Peng, Y.; Pan, F.; Li, J.; Zou, L.; Zhang, Y.; Liang, H. HIF-1α inhibition reverses multidrug resistance in colon cancer cells via downregulation of MDR1/P-glycoprotein. *PLoS ONE* **2014**, *9*, e98882. [CrossRef] [PubMed]

34. Wartenberg, M.; Richter, M.; Datchev, A.; Grünther, S.; Milosevic, N.; Bekhite, M.M.; Figulla, H.R.; Aran, J.M.; Pétriz, J.; Sauer, H. Glycolytic pyruvate regulates P-Glycoprotein expression in multicellular tumor spheroids via modulation of the intracellular redox state. *J. Cell. Biochem.* **2010**, *109*, 434–446. [CrossRef] [PubMed]

35. Bitting, R.L.; Armstrong, A.J. Targeting the PI3K/Akt/mTOR pathway in castration-resistant prostate cancer. *Endocr. Relat. Cancer* **2013**, *20*, R83–R99. [CrossRef] [PubMed]

36. Wu, L.; Birle, D.C.; Tannock, I.F. Effects of the mammalian target of rapamycin inhibitor CCI-779 used alone or with chemotherapy on human prostate cancer cells and xenografts. *Cancer Res.* **2005**, *65*, 2825–2831. [CrossRef] [PubMed]

37. Hambright, H.G.; Meng, P.; Kumar, A.P.; Ghosh, R. Inhibition of PI3K/AKT/mTOR axis disrupts oxidative stress mediated survival of melanoma cells. *Oncotarget* **2015**, *6*, 7195–7208. [CrossRef] [PubMed]

38. Hager, S.; Ackermann, C.J.; Joerger, M.; Gillessen, S.; Omlin, A. Anti-tumor activity of platinum compounds in advanced prostate cancer-a systematic literature review. *Ann. Oncol.* **2016**, *27*, 975–984. [CrossRef] [PubMed]

39. Marullo, R.; Werner, E.; Degtyareva, N.; Moore, B.; Altavilla, G.; Ramalingam, S.S.; Doetsch, P.W. Cisplatin induces a mitochondrial-ROS response that contributes to cytotoxicity depending on mitochondrial redox status and bioenergetic functions. *PLoS ONE* **2013**, *8*, e81162. [CrossRef] [PubMed]

40. Hervault, A.; Thanh, N.T. Magnetic nanoparticle-based therapeutic agents for thermo-chemotherapy treatment of cancer. *Nanoscale* **2014**, *6*, 11553–11573. [CrossRef] [PubMed]